SUPPORTIN INFORMATION

Tailor-made Block Copolymers of L-, D-, *rac*-Lactides and ε-Caprolactone *via* One-Pot Sequential Ring Opening Polymerization by Pyridylamidozinc(II) Catalysts

Ilaria D'Auria,[a] Massimo Christian D'Alterio,[b] Consiglia Tedesco[a] and Claudio Pellecchia*[a]

[a] Dipartimento di Chimica e Biologia "A. Zambelli", Università di Salerno, via Giovanni Paolo II 132, 84084 Fisciano (SA), Italy.

[b] Dipartimento di Scienze Chimiche, Università "Federico II" di Napoli, Complesso Monte Sant'Angelo, via Cintia 21, 80126 Napoli, Italy.

Table of contents

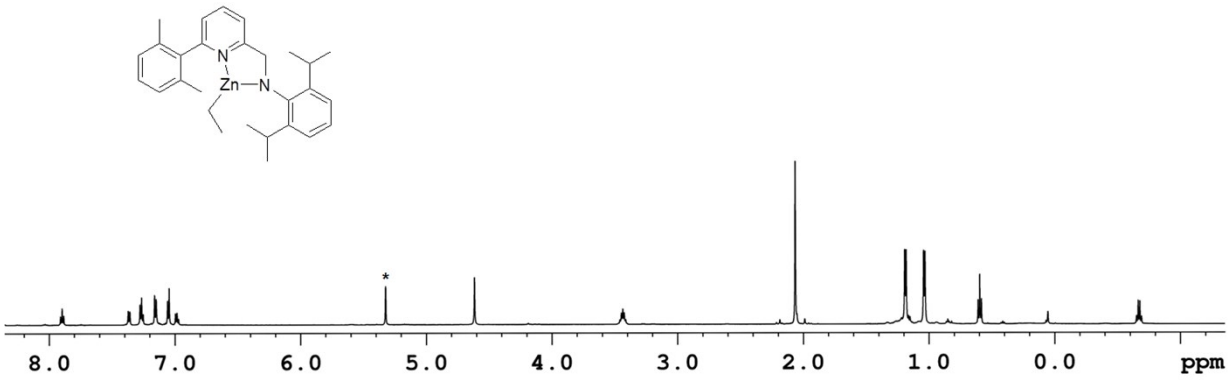

Figure S1. ^{1}H-NMR (CD_2Cl_2, 600 MHz, 25°C) of complex **L^{1}ZnEt** (* stands for residual solvent resonances).

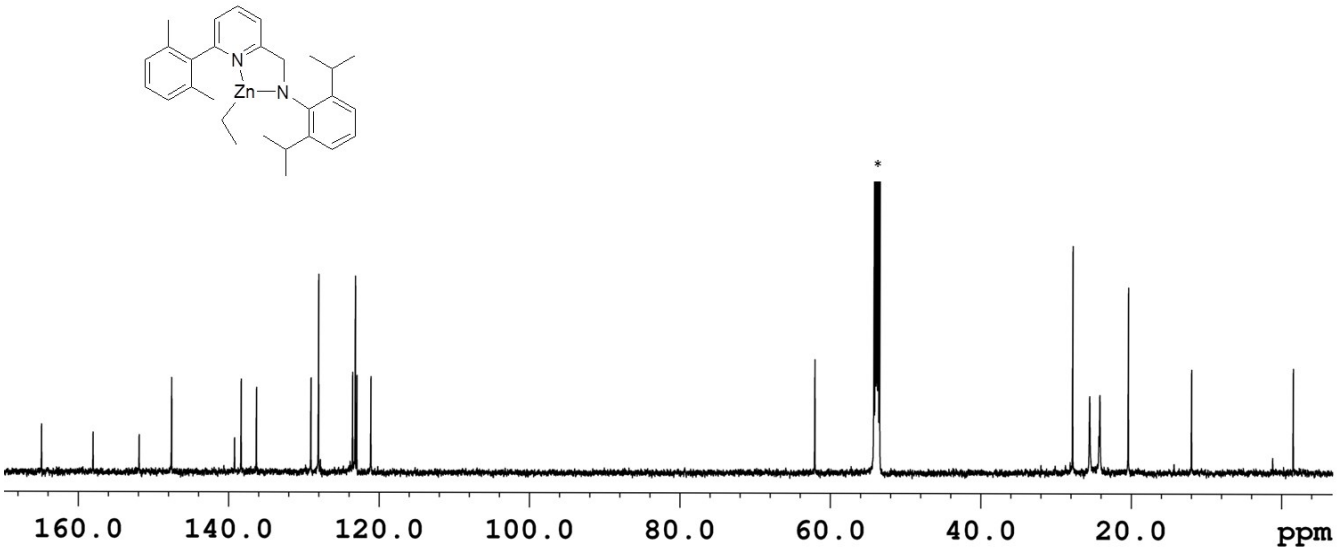

Figure S2. ^{13}C-NMR (CD_2Cl_2, 150 MHz, 25°C) of complex **L^{1}ZnEt** (* stands for residual solvent resonances).

X-ray crystallography

A suitable crystal of **L^1ZnEt** was selected and mounted on a cryoloop with paratone oil and measured at 100 K with a Rigaku AFC7S diffractometer equipped with a Mercury2 CCD detector using graphite monochromated MoKα radiation (λ = 0.71069 Å). Data reduction was performed with the crystallographic package CrystalClear.[1] Data were corrected for Lorentz, polarization and absorption.

A suitable crystal of **L^3Zn(SiMe$_3$)$_2$** was inserted in a 0.4 mm Lindemann and measured at room temperature with a Bruker D8 QUEST diffractometer equipped with a PHOTON100 detector using CuKα radiation (λ= 1.54178 Å). Indexing was performed using APEX3.[2] Data integration and reduction were performed using SAINT.[2] Absorption correction was performed by multi-scan method in SADABS.[2] For both compounds the structures were solved by Direct Methods using SIR2014[3] and refined by means of full matrix least-squares based on F2 using the program SHELXL.[4] For both compounds non-hydrogen atoms were refined anisotropically, hydrogen atoms were positioned geometrically and included in structure factors calculations, but not refined. Crystal data and refinement details are reported in Table S1. Crystal structures were drawn using OLEX2.[5]

In **L^1ZnEt** the Zn atom deviates by -0.068(18) Å from the triangle mean plane defined by N1, N2 and C27 atoms. In **L^3ZnN(SiMe$_3$)$_2$** the Zn atom deviates by 0.065(14) Å from the triangle mean plane defined by N1, N2 and N3 atoms. Both pyridylamido ligands display an almost perfect planar geometry within a rmsd of 0.0009 Å and 0.043 Å, respectively for **L^1ZnEt** and **L^3ZnN(SiMe$_3$)$_2$**. In both compounds the alkyl substituted aromatic moieties are perpendicular to the bidentate ligand plane. In detail, the isopropyl substituted aromatic moieties are tilted by 86.8(4)° and 79.19(12)°, respectively, while the methyl substituted aromatic moieties are tilted by 74.6(4)° and 62.81(0.12)°, respectively. In both compounds amido nitrogen atoms N1 feature the shortest distances with the zinc atom, 1.867(8) Å and 1.857(2) Å, respectively, while pyridine nitrogen atoms N2 the longest distances with the zinc atom, 2.078(8) Å and 2.146 Å.

Table S1. Crystallographic data and refinement details for compounds **L^1ZnEt** and **$L^3Zn(SiMe_3)_2$**

	L^1ZnEt	**$L^3Zn(SiMe_3)_2$**
T (K)	100	296
Crystal size (mm x mm x mm)	0.44 x 0.32 x 0.27	0.55 x 0.36 x 0.26
Formula	$C_{28}H_{36}N_2Zn$	$C_{33}H_{51}N_3Si_2Zn$
Formula weight	465.96	611.33
System	triclinic	monoclinic
Space group	$P\bar{1}$	$P2_1/c$
***a* (Å)**	8.671(4)	13.188(4)
***b* (Å)**	8.736(3)	10.266(4)
***c* (Å)**	19.457(10)	26.260(16)
***α* (°)**	78.79(3)	90
***β* (°)**	84.49(4)	93.00(3)
***γ* (°)**	67.01(3)	90
***V* (Å^3)**	1330.6(11)	3550(3)
Z	2	4
D_x (g cm^{-3})	1.163	1.144
λ (Å)	0.71073	1.54178
μ (mm^{-1})	0.938	1.774
F_{000}	496	1312
***R*1 (I > 2σI)**	0.1157 (1535)	0.0361 (3604)
$_wR_2$ (all data)	0.4084 (6042)	0.0989 (4073)
N. of param.	286	365
GooF	0.994	1.035
ρ_{min}, ρ_{max} (eÅ^{-3})	-0.425, 0.400	-0.361, 0.276

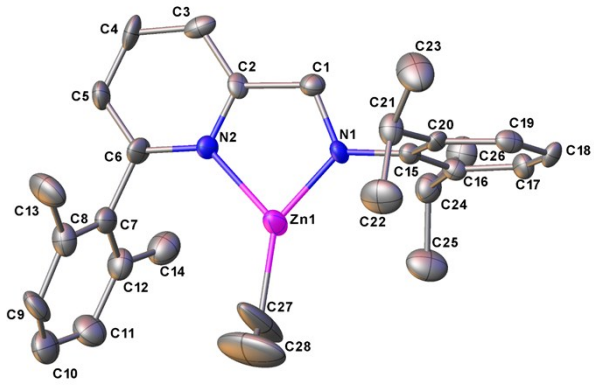

Figure S3. Ortep drawing of **L[1]ZnEt**. Hydrogen atoms have been omitted for clarity. Ellipsoids are drawn at 15% probability level.

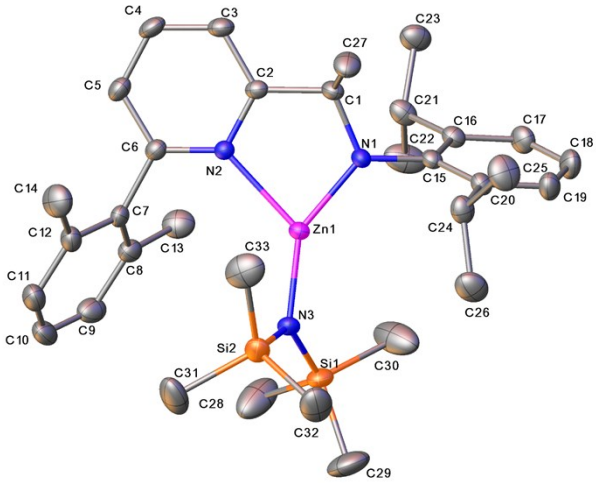

Figure S4. Ortep drawing of **L[3]ZnN(SiMe$_3$)$_2$**. Hydrogen atoms have been omitted for clarity. Ellipsoids are drawn at 20% probability level.

Table S2. Selected bond distances (Å) and bond angles (°) for **L[1]ZnEt** and **L[3]ZnN(SiMe$_3$)$_2$**

L[1]ZnEt		**L[3]ZnN(SiMe$_3$)$_2$**	
Zn1—N1	1.867(8)	Zn1—N1	1.857(2)
Zn1—N2	2.078(8)	Zn1—N2	2.146(2)
Zn1— C27	1.99(2)	Zn1—N3	1.873(2)
N1—Zn1— N2	83.7(4)	N1—Zn1—N2	83.46(9)
N1—Zn1— C27	146.4(9)	N1—Zn1—N3	145.20(10)
C27—Zn1— N2	129.5(8)	N3—Zn1—N2	130.93(9)

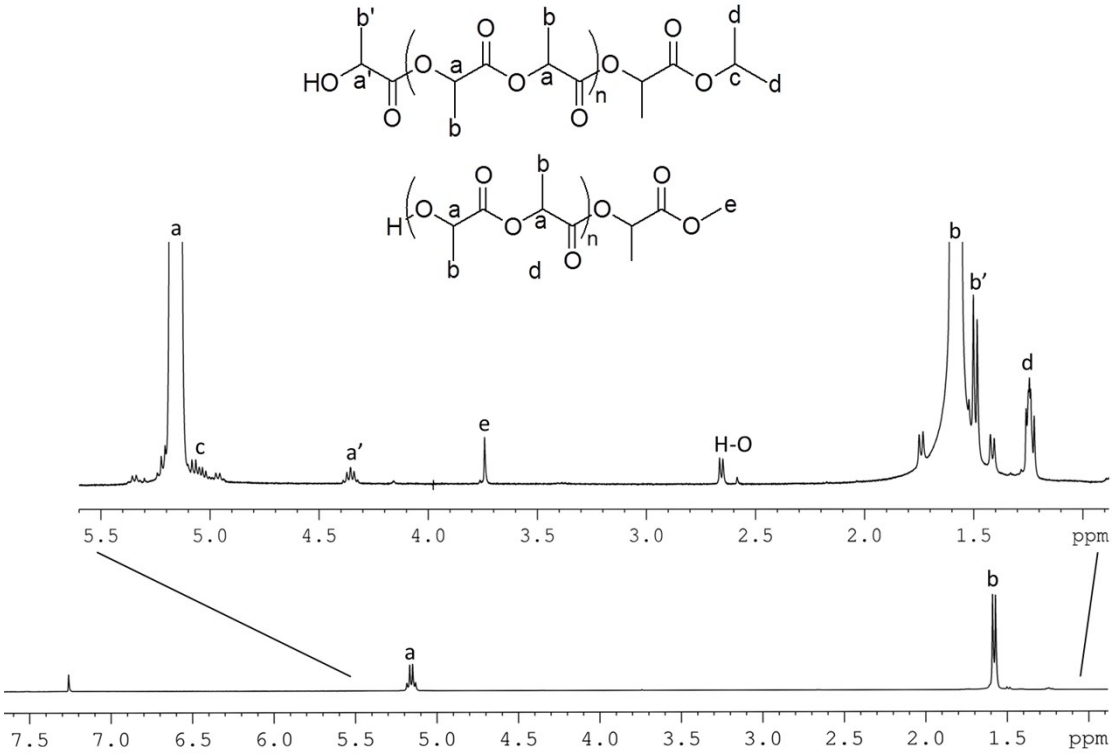

Figure S5. ^{1}H-NMR ($CDCl_3$, 400 MHz, 298 K) of a low molecular weight PLA sample prepared using **$L^2ZnN(SiMe_3)_2$** as catalyst in dichloromethane at 25°C.

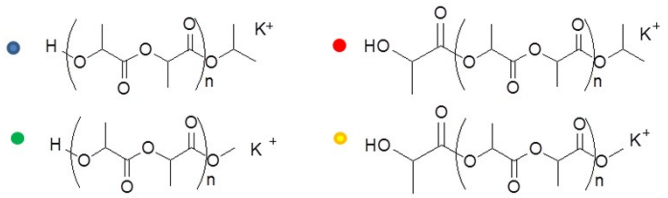

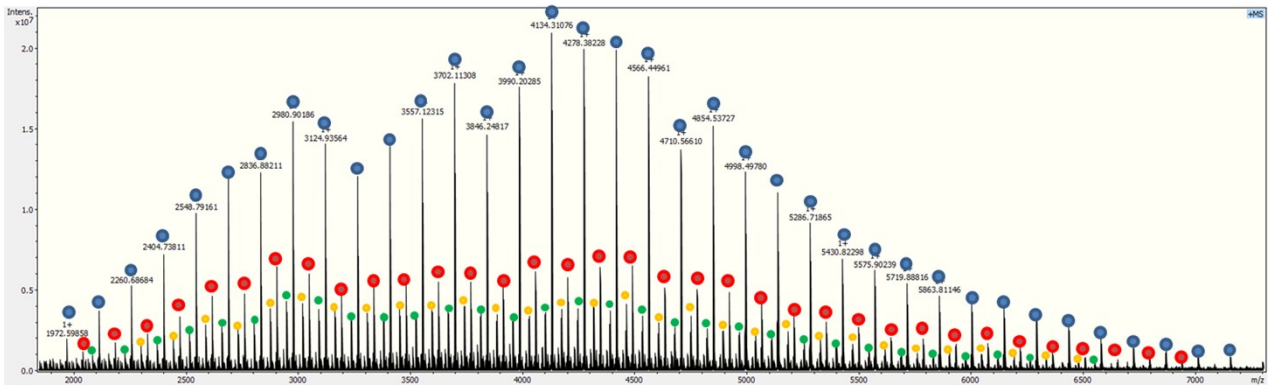

Figure S6. MALDI-TOF mass spectrum (doped with K^+) of a low molecular weight PLA sample prepared using **$L^2ZnN(SiMe_3)_2$ / *i*PrOH** 1:1, in dichloromethane at 25°C.

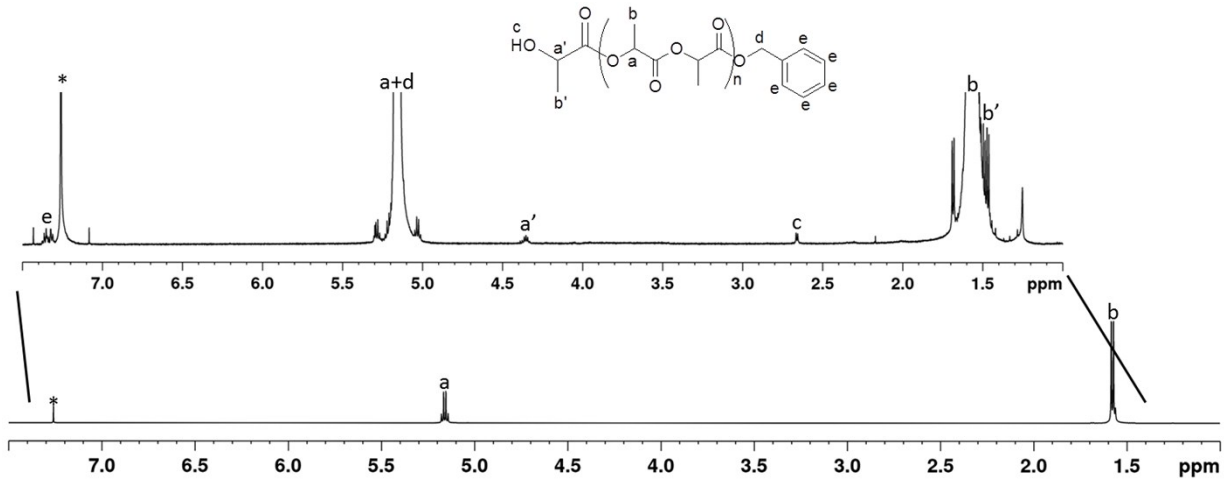

Figure S7. ^{1}H-NMR ($CDCl_3$, 400 MHz, 298 K) of PLA sample obtained in run 18 of Table 1 (* stands for residual solvent resonances).

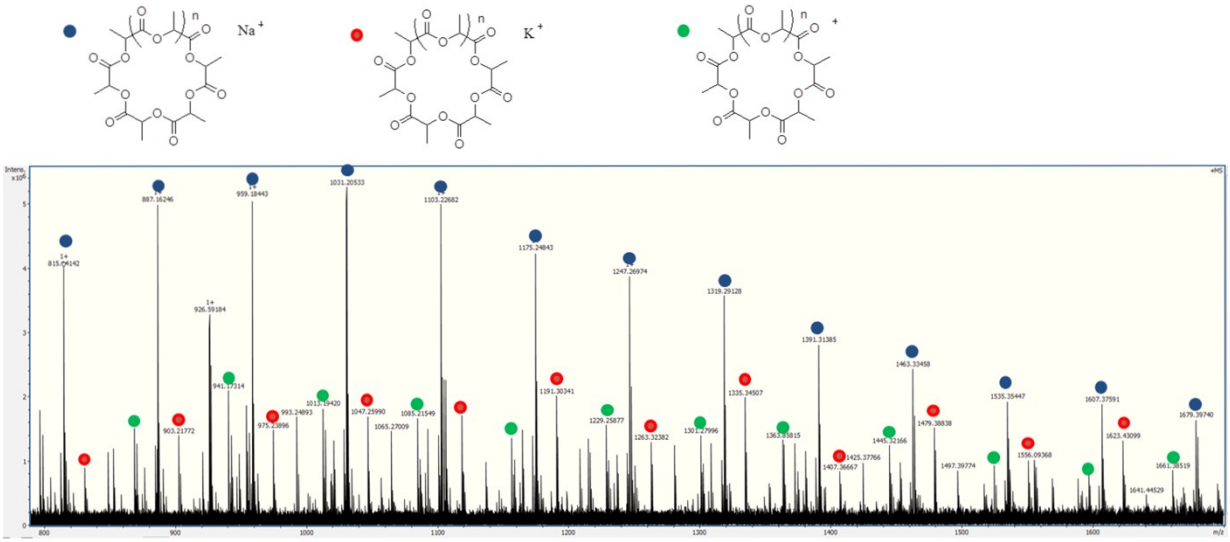

Figure S8. MALDI-TOF mass spectrum of low-molecular weight fraction of PLA sample (run 18, Table 1) in the m/z range: 750 – 1700. Blue circle labelled series calculated for $[(C_3H_4O_2)_n + (C_3H_4O_2)_5 + Na]^+$; red circle labelled series calculated for $[(C_3H_4O_2)_n + [(C_3H_4O_2)_5 + K]^+$ and green circle labelled series calculated for $[(C_3H_4O_2)_n + [(C_3H_4O_2)_5\ ]^+$, with n between 6 and 18 units.

Table S3. SEC analysis of the block copolymers of LLA, DLA, DLLA and ε-CL[a]

		1 block		2 blocks		3 blocks		4 blocks	
Run	copolymer [theoretical block length]	M_{nSEC}[b] (M_{nTHEO})[c] [kDa]	M_w/M_n[b]	M_{nSEC}[b] (M_{nTHEO})[c] [kDa]	M_w/M_n[b]	M_{nSEC}[b] (M_{nTHEO})[c] [kDa]	M_w/M_n[b]	M_{nSEC}[b] (M_{nTHEO})[c] [kDa]	M_w/M_n[b]
26	PLLA-*b*-PDLA [100-*b*-100]	13.5 (14.3)	1.3	18.8 (27.6)	1.2	-	-	-	-
27	PLLA-*b*-PDLA [200-*b*-200]	nd	nd	41.1 (55.3)	1.2	-	-	-	-
28	PLLA-*b*-PDLA-*b*-PLLA [100-*b*-100-*b*-100]	14.7 (14.3)	1.4	24.9 (28.5)	1.1	36.8	1.1	-	-
29	PLLA-*b*-PDLLA-*b*-PDLA [100-*b*-100-*b*-100]	15.6 (14.3)	1.4	28.2 (28.5)	1.3	34.4 (40.2)	1.2	-	-
30	PLLA-*b*-PDLA-*b*-PLLA-*b*-PDLA [100-*b*-100-*b*-100-b-100]	n.d.[d]	n.d.	n.d.	n.d.	n.d.	n.d.	37.8 (55.3)	1.2
31	PCL-*b*-PDLA [200-*b*-200]	17.5 (12.8)	1.3	27.5 (31.8)	1.4	-	-	-	-

[a]Polymerizations performed in CH_2Cl_2 [2 mL] at 25°C employing 10 μmol of [$L^2ZnN(SiMe_3)_2$] and 1 equiv of *i*PrOH. Full conversion was confirmed by ^1H NMR. 20–30 min was maintained between each monomer addition, depending on the monomer amount and length of polymer chain. [b]Experimental Mn [in g mol^{-1}] and M_w/M_n values determined by SEC in THF against polystyrene standards, using the correction factor 0.58 for lactide and 0.56 for caprolactone. [c]M_{nTHEO} (in g mol^{-1}) = 144.13 × $([LA]_0)/([Zn]_0)$ × conversion LA. M_{nTHEO} (in g mol^{-1}) = 114.14 × $([\varepsilon CL]_0)/([Zn]_0)$ × conversion ε-CL. [d]Not determined. Since the polymerizations must be performed under strictly inert atmosphere, intermediate sampling was done for the diblock and the triblock copolymers, but not for the tetrablock one.

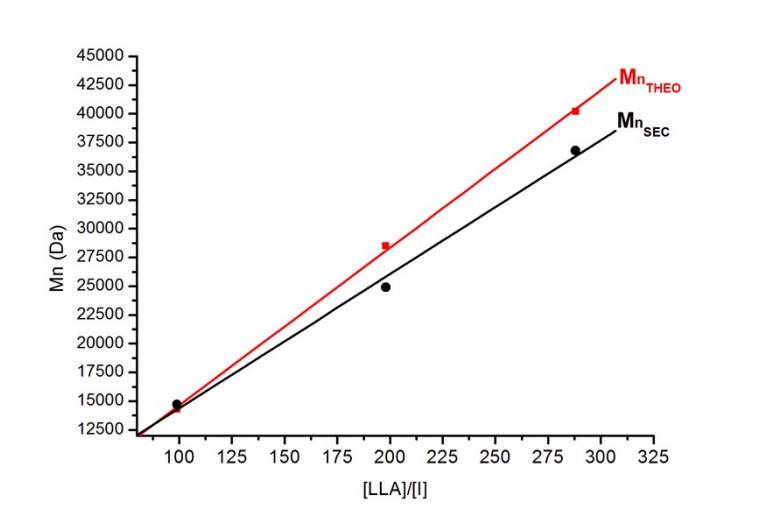

Figure S9. Plot of number-average molecular weights from SEC (black) and theoretical (red) vs monomer-to-initiator ratio [LA] /[I] for triblock PLLA-*b*-PDLA-*b*-PLLA (run 28, Table S2).

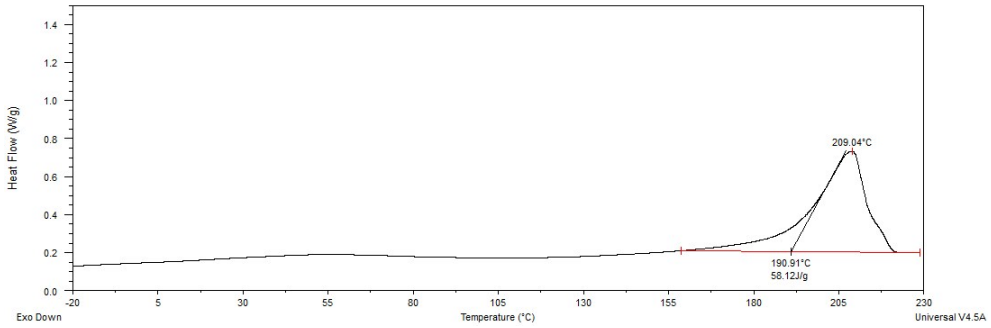

Figure S10. Thermogram of first DSC heating run of diblock copolymer LLA-*b*-DLA, 100-*b*-100, run 26, Table 3.

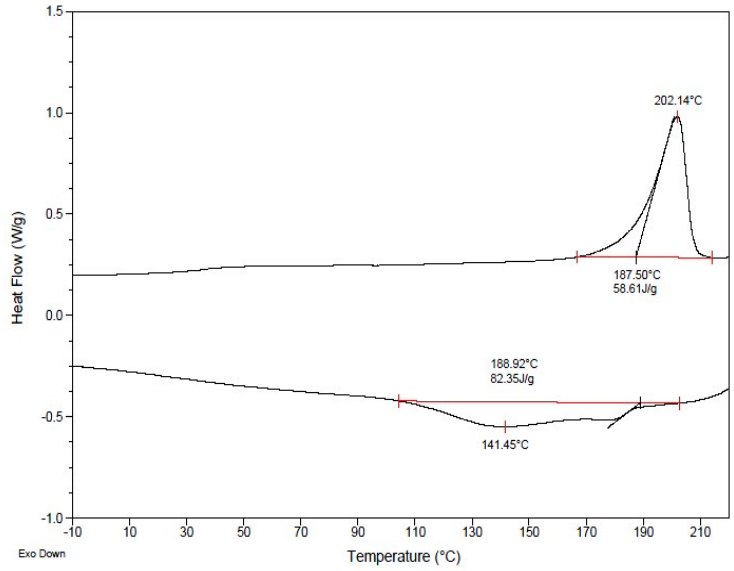

Figure S11. Thermograms of second DSC heating (up) and cooling (bottom) run of diblock copolymer LLA-*b*-DLA, 100-*b*-100, run 26, Table 3.

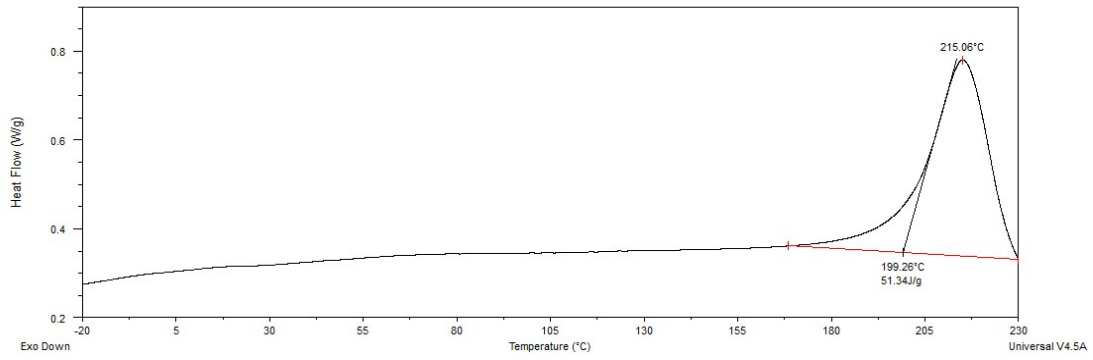

Figure S12. Thermogram of first DSC heating run of diblock copolymer LLA-DLA, 200-*b*-200, run 27, Table 3.

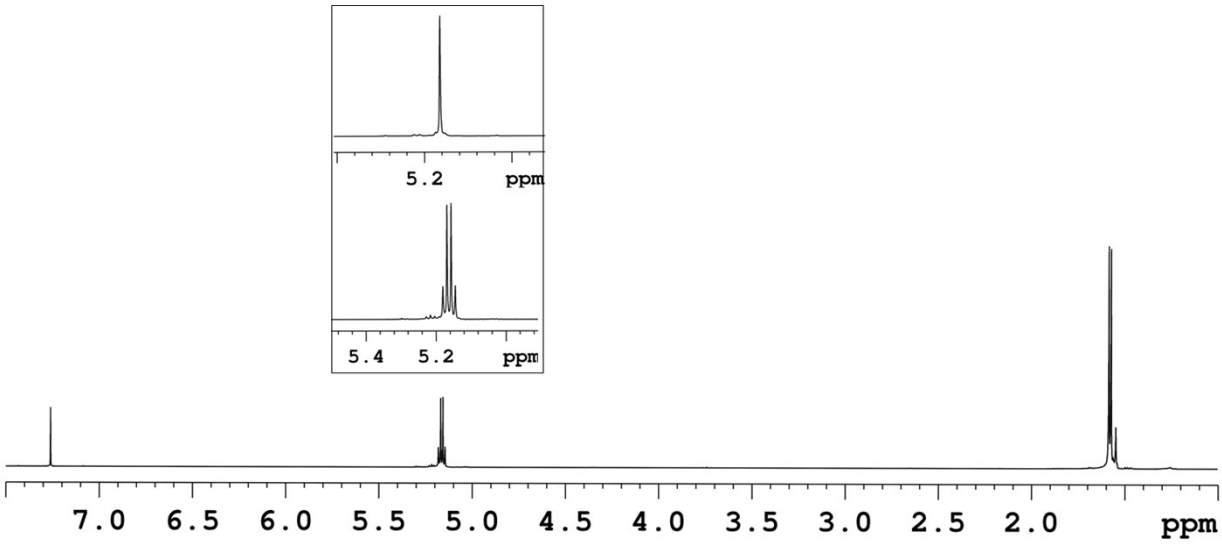

Figure S13. ^{1}H-NMR and HD-NMR (square) ($CDCl_3$, 600MHz) of LLA-DLA-LLA, 100-*b*-100-*b*-100, triblock PLA copolymer sample (run 28, Table 3).

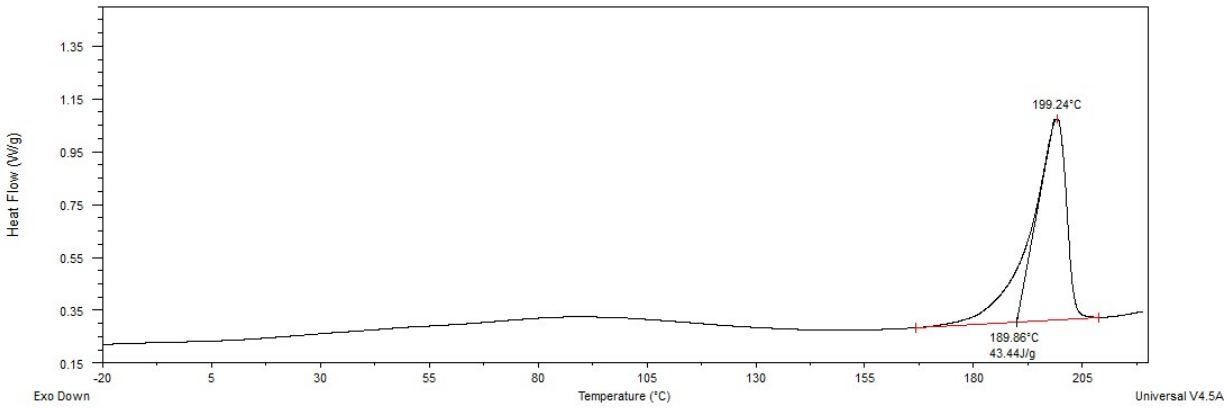

Figure S14. Thermogram of first DSC heating run of triblock copolymer LLA-*b*-DLA-*b*-LLA, run 28, Table 3.

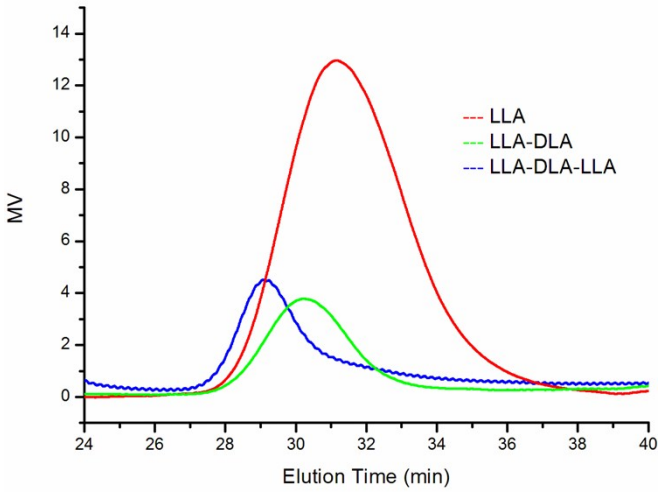

Figure S15. SEC profiles of triblock copolymer LLA-*b*-DLA-*b*-LLA, run 28, Table 3.

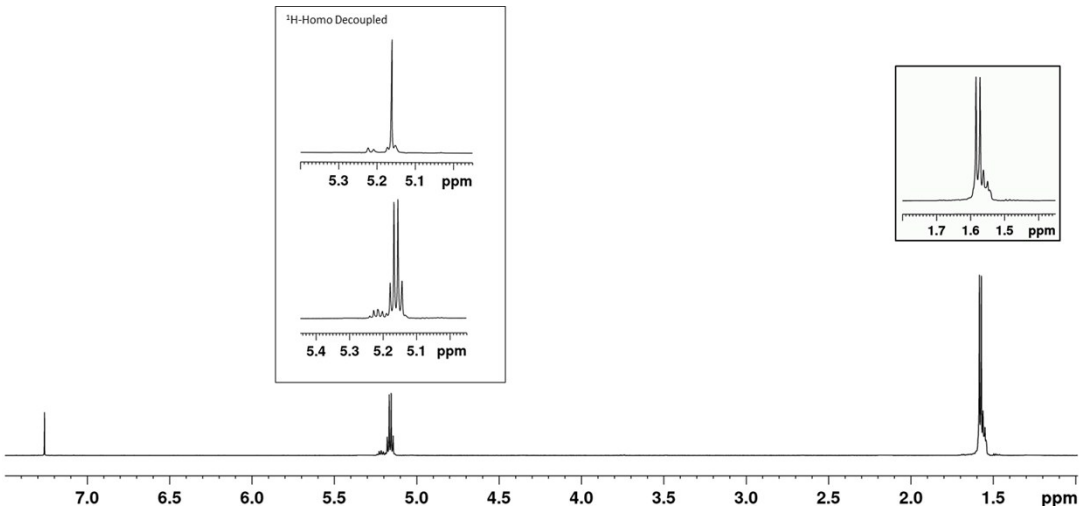

Figure S16. ^{1}H-NMR and HD-NMR ($CDCl_3$, 600MHz) of LLA-DLLA-LLA, 100-*b*-100-*b*-100, triblock PLA copolymer sample (run 29, Table 3).

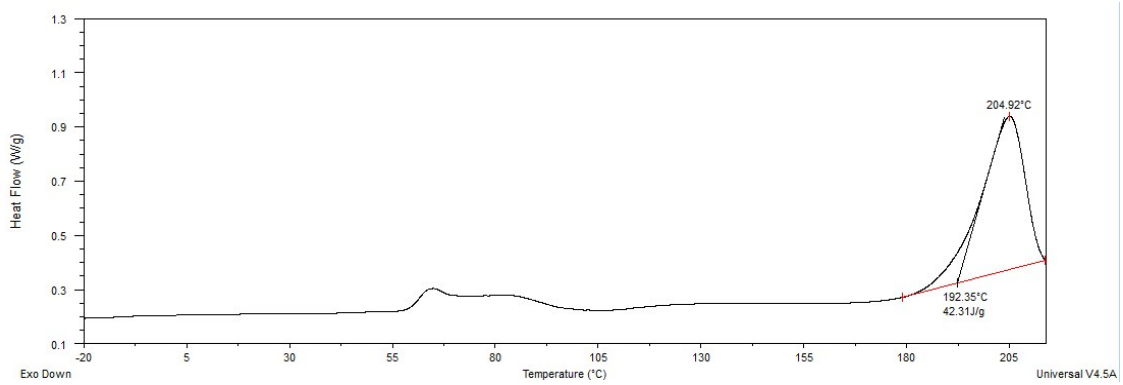

Figure S17. Thermogram of first DSC heating run of triblock copolymer LLA-*b*-DLLA-*b*-LLA, run 29, Table 3.

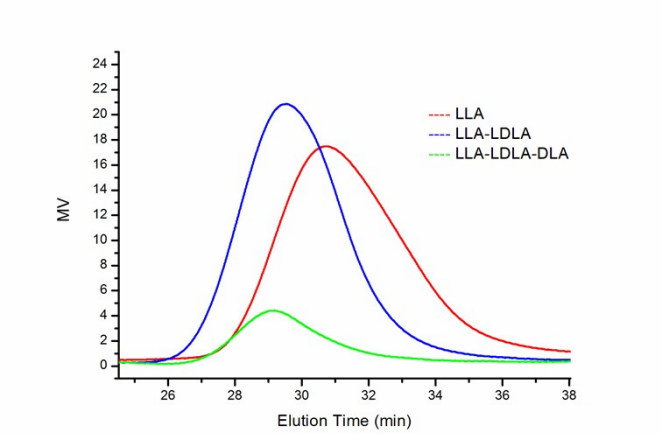

Figure S18. SEC profiles of triblock copolymer LLA-DLLA-LLA, 100-*b*-100-*b*-100 in run 29 of Table 3.

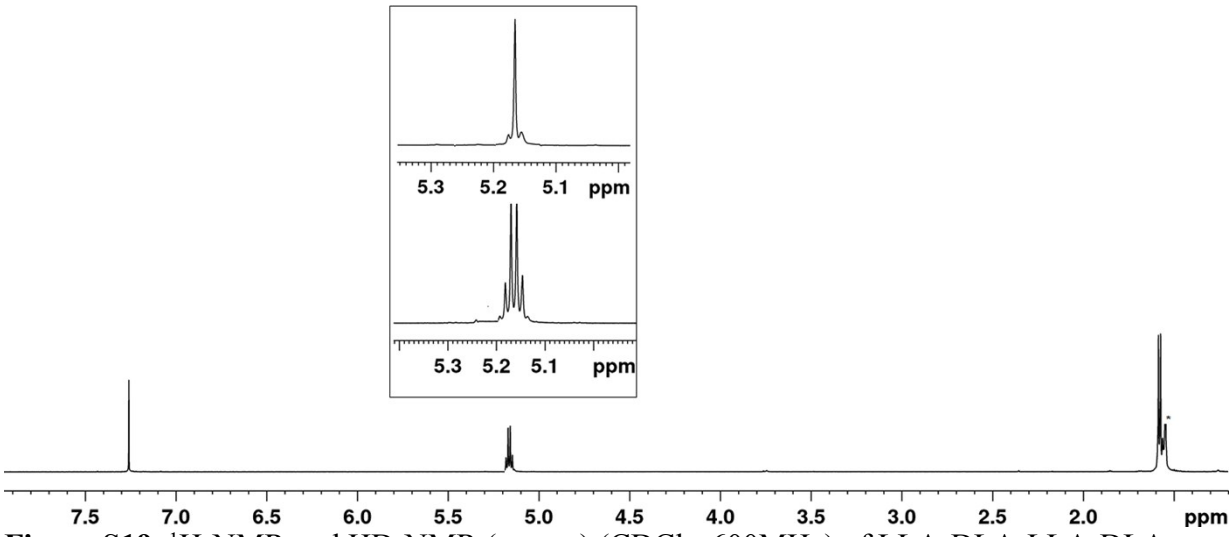

Figure S19. ^{1}H-NMR and HD-NMR (square) ($CDCl_3$, 600MHz) of LLA-DLA-LLA-DLA, 100-*b*-100-*b*-100-B-100, tetrablock PLA copolymer sample (run 30, Table 3), (* stands for residual solvent resonances).

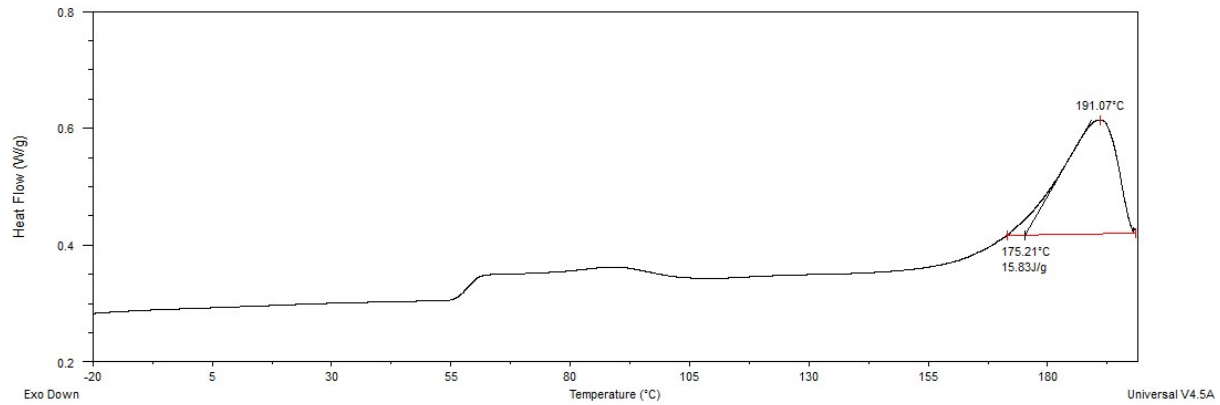

Figure S20. Thermogram of first DSC heating run of tetrablock copolymer LLA-*b*-DLA-*b*-LLA-*b*-DLA, run 30, Table 3.

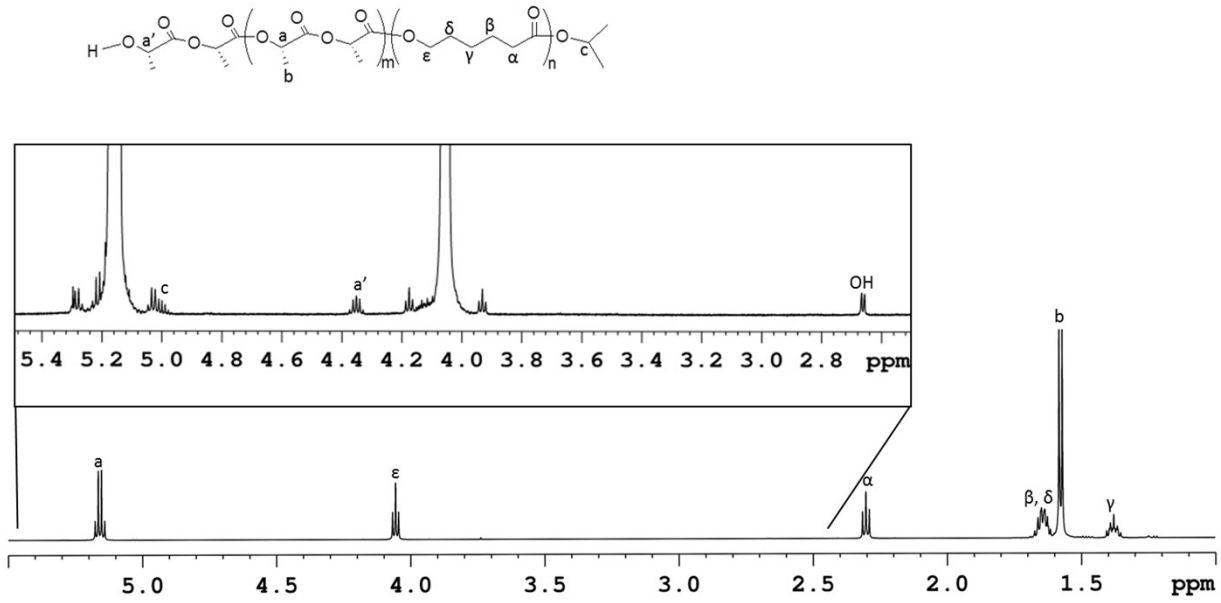

Figure S21. ^{1}H-NMR ($CDCl_3$, 600MHz) of PCL-LLA, 200-*b*-200, diblock copolymer sample (run 31, Table 3).

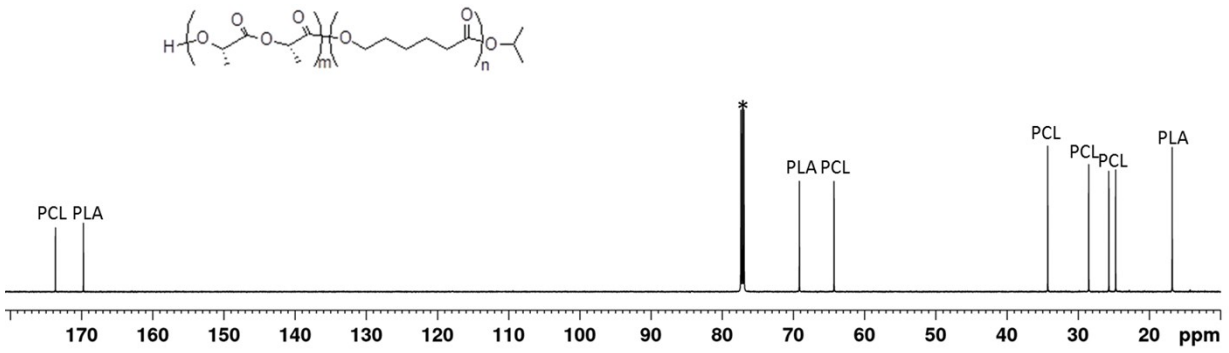

Figure S22. ^{13}C-NMR ($CDCl_3$, 150MHz) of PCL-LLA, 200-*b*-200, diblock copolymer sample (run 31, Table 3).

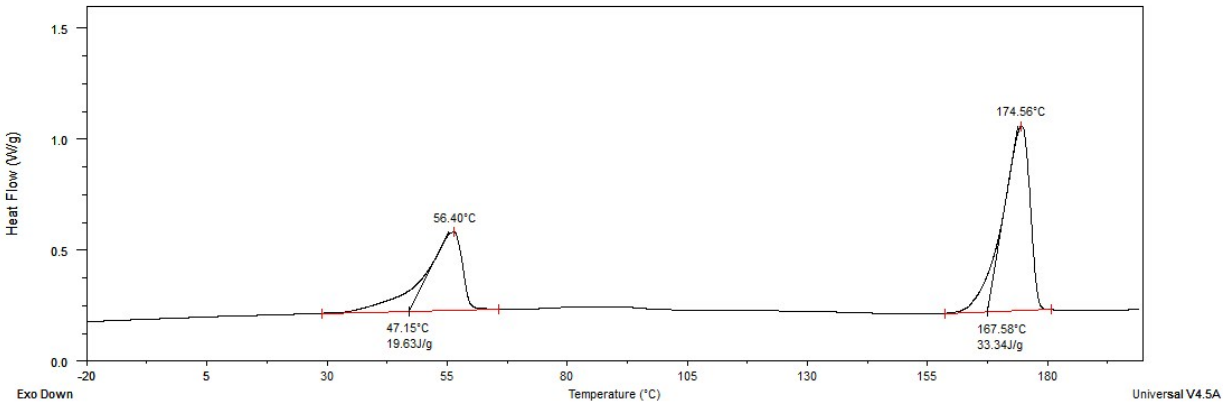

Figure S23. Thermogram of first DSC heating run of diblock copolymer CL-*b*-LLA, run 31, Table 3.

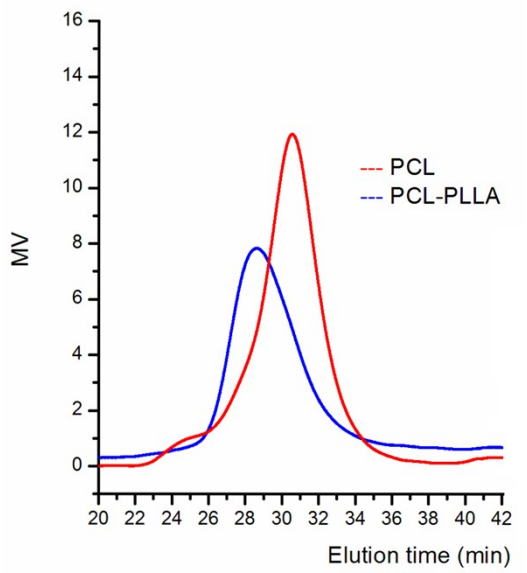

Figure S24. SEC profiles of diblock copolymerPCL-PLA copolymer in run 31 of Table 3.

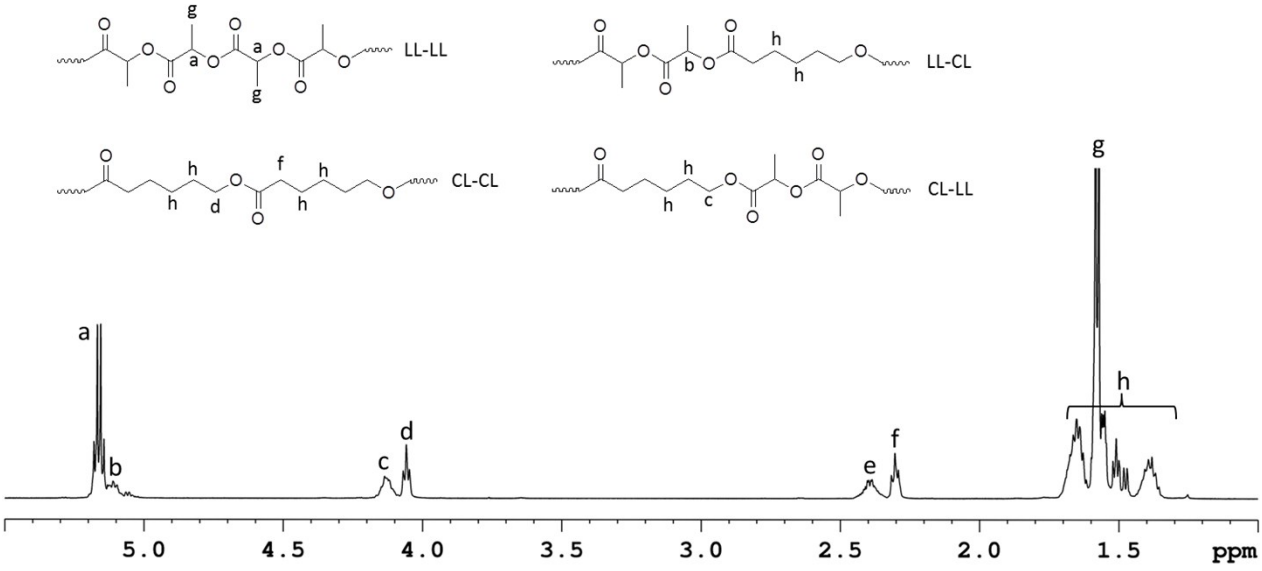

Figure S25. ^{1}H-NMR ($CDCl_3$, 600MHz) of a random copolymer sample of Cl and LLA.

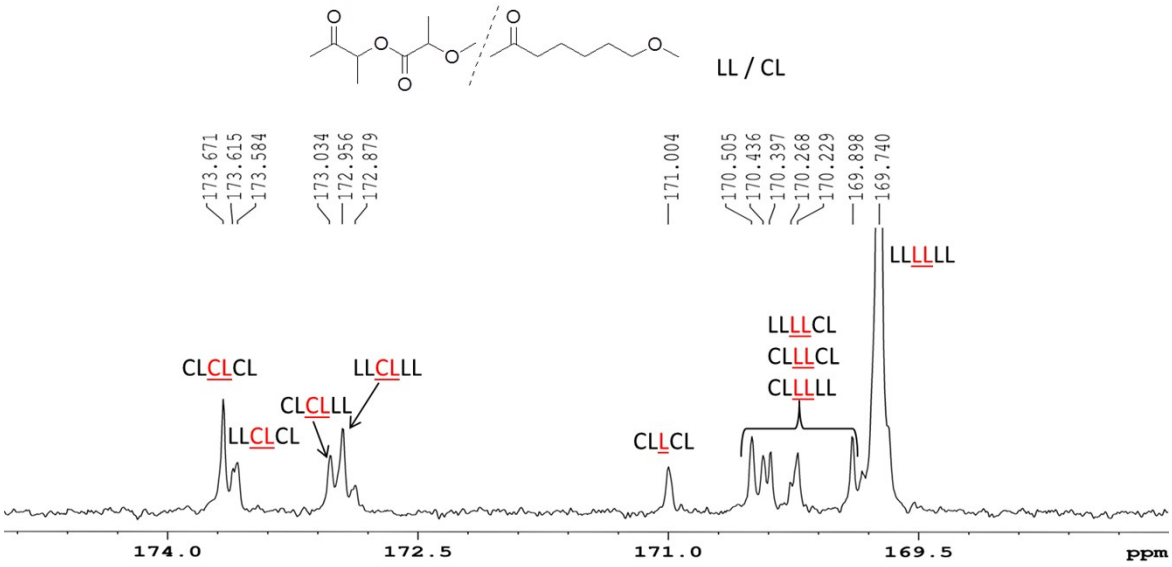

Figure S26. Carbonyl region of the ^{13}C NMR (150 MHz, $CDCl_3$) spectrum of a random copolymer sample of Cl and LLA.

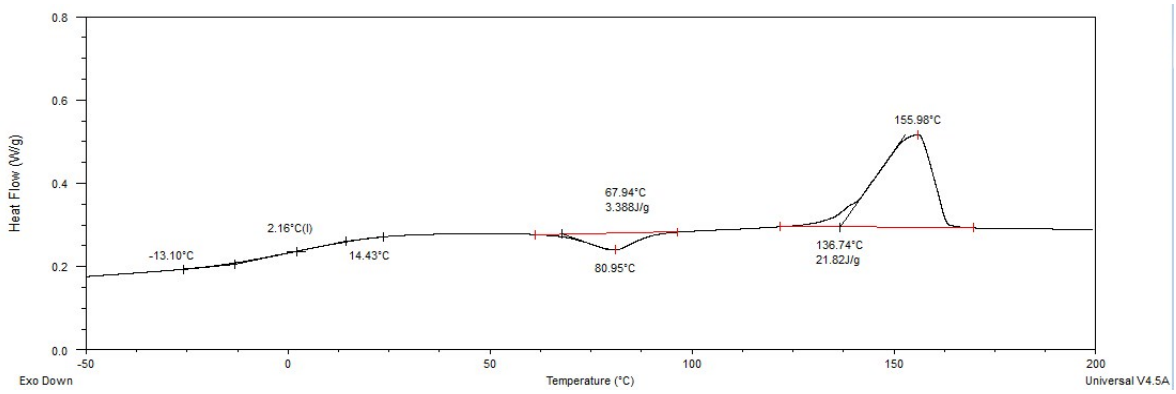

Figure S27. Thermogram of first DSC heating run of a random copolymer sample of Cl and LLA.

References

1. CrystalClear, Crystal Structure Analysis Package, Rigaku-Molecular Structure Corp.
2. APEX3, SAINT, SADABS. Bruker AXS Inc., Madison, Wisconsin, USA. Bruker AXS Inc., Madison, Wisconsin, USA, 2012.
3. Burla, M. C.; Caliandro, R.; Carrozzini, B.; Cascarano, G. L.; Cuocci, C.; Giacovazzo, C.; Mallamo, M.; Mazzone, A.; Polidori, G. Crystal structure determination and refinement via SIR2014. J. Appl. Cryst. 2015, 48, 306-309.
4. Sheldrick, G. M. Crystal structure refinement with SHELXL. Acta Cryst. 2015, C71, 3–8.
5. Dolomanov, O. V.; Bourhis, L. J.; Gildea, R. J.; Howard, J. A. K.; Puschmann, H. OLEX2: a complete structure solution, refinement and analysis program. J. Appl. Cryst. 2009, 42, 339–341.